Bulletin of the Seismological Society of America, 91, 5, pp. 953–958, October 2001

Influence of Surface-Normal Ground Acceleration on the Initiation of the Jih-Feng-Erh-Shan Landslide during the 1999 Chi-Chi, Taiwan, Earthquake

by Chien-Cheng Huang, Yuan-Hsi Lee, Hsi-Ping Liu, David K. Keefer, and Randall W. Jibson

Abstract The 1999 Chi-Chi, Taiwan, earthquake triggered numerous landslides throughout a large area in the Central Range, to the east, southeast, and south of the fault rupture. Among them are two large rock avalanches, at Tsaoling and at Jih-Feng-Erh-Shan. At Jih-Feng-Erh-Shan, the entire thickness (30–50 m) of the Miocene Changhukeng Shale over an area of 1 km^2 slid down its bedding plane for a distance of about 1 km. Initial movement of the landslide was nearly purely translational. We investigate the effect of surface-normal acceleration on the initiation of the Jih-Feng-Erh-Shan landslide using a block slide model. We show that this acceleration, currently not considered by dynamic slope-stability analysis methods, significantly influences the initiation of the landslide.

Basic Earthquake Data

The earthquake occurred at 17:47, 20 September 1999 (UTC), (1:47 a.m., 21 September 1999 local time) with a moment magnitude $\mathbf{M}_w$ 7.6. The epicenter was located at (23.87° N, 120.75° E) with a focal depth of ~7 km (Ma *et al.,* 1999). An earthquake focal mechanism was given as strike = 357° and dip = 29° (Shin *et al.,* 2000). The earthquake was generated by an oblique thrust motion on the Chelungpu fault, and the amount of fault slip increased from tens of centimeters in the south to about 10 m in the north. The Chelungpu fault is one of a series of north- to northeast-trending imbricate thrust faults dipping to the east (Ho, 1988). Approximately 650 three-component strong-motion digital accelerometers were deployed at free-field sites prior to the Chi-Chi earthquake (Fig. 1). Records of the Chi-Chi earthquake from more than 400 instruments have been successfully retrieved and distributed on compact discs (Lee *et al.,* 1999). Amplitudes of ground acceleration are significantly higher along the Chelungpu fault and on the hanging-wall block of the fault than at other locations.

Introduction

The earthquake triggered two very large landslides (Central Geological Survey, 2000). These are the complex rock-block slide avalanches at Tsaoling and at Jih-Feng-Erh-Shan. Both began as translational rock-block slides on dip slopes, and both disintegrated during movement into highly disrupted rock avalanches that traveled long distances at evidently high velocities.

The rock avalanche at Tsaoling (about 29 km south-southwest from the town of Chi-Chi, see Fig. 2) affected an area of over 5 km^2 involving about 120 × 10^6 m^3 of material. It originated on a dip slope on the north side of the Ching-Shui River, which has been undercutting the toe of the slope for at least several decades. Similar large landslides occurred from the same slope and in the same Cholan Formation in 1862, 1941, 1942, and in 1979 (Central Geological Survey, 2000). The 1862 and 1941 landslides were triggered by earthquake (*M* 6–7 and *M* 7.1, respectively), while the 1942 and 1979 landslides were associated with heavy rainfall. Rock making up the landslide consists of Pliocene to Pleistocene weakly cemented argillaceous sandstone, shale, and siltstone.

The rock slide-avalanche at Jih-Feng-Erh-Shan occurred in the epicentral area about 16 km north-northeast from the town of Chi-Chi (Fig. 2). A layer, 30–50 m thick, of the Miocene Changhukeng Shale (shale interbedded with thin sandstone layers) over an area of 1 km^2 slid down the bedding plane separating the Changhukeng Shale from the underlying Shihmen Formation (thick sandstone) toward the southeast for a distance of about 1 km. The slide surface strikes N40° E and dips between 18° and 24° toward the southeast. A volume of over 30 × 10^6 m^3 of material was involved in the slide (Central Geological Survey, 2000). Kamai *et al.* (2000) reported that the number of deaths caused by the landslide to be 90. Figure 3 shows the geology and stream pattern (before this earthquake) of the area. A photograph of a rockslide at the northern end of the landslide is shown in Figure 4. Rock exposed in the crown and head scarp area is broken by a set of prominent, planar joints with dips near vertical and strikes parallel to the scarp. A layer of clayey material exposed at the joint surface at the head scarp indicates the joints were open prior to the movement. A synclinal axis (the Ta-An-Shan Syncline) with previous tectonic displacements along it lies at the foot of the landslide. The Sezikeng and the Jiutsaihu streams had undercut

Figure 1. Locations of the free-field, three-component, digital accelerometer stations. The star indicates the location of the mainshock. Surface ruptures extending about 80 km in a nearly north–south direction are shown by the jagged line to the left of the mainshock (from Lee *et al.,* 1999).

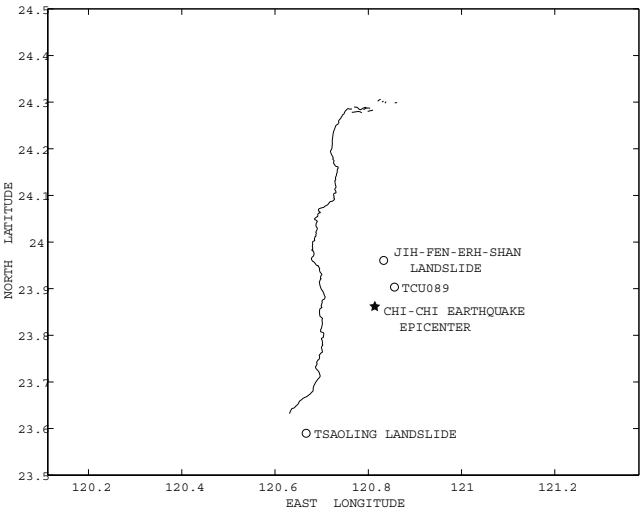

Figure 2. Location of the Tsaoling and Jih-Feng-Erh-Shan landslides and strong-motion station TCU089 discussed in the text.

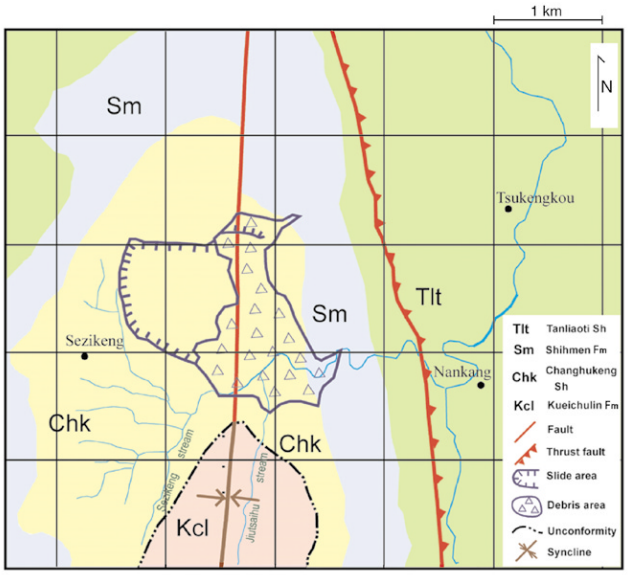

Figure 3. Geology and stream pattern (before the Chi-Chi earthquake) in the area of the Jih-Feng-Erh-Shan landslide (modified from Central Geological Survey, 2000, p. 94). A fault extends across the toe of the landslide (note the 590-m displacement immediately north of the landslide). The fault movement stopped after the deposition of Kcl and became a syncline.

the toe of the landslide prior to the earthquake. The preexisting open joint at the head scarp suggests that the block that slid was under tension prior to the earthquake and that incipient movement of material had occurred near the head scarp, opening tension fractures long before the earthquake triggered large slope failure. It is most likely that that rock block was kept from sliding before the earthquake mainly by basal friction.

Because the slide direction coincides with the dip of the underlying surface, and because the entire formation was involved, initial movement is inferred to be nearly pure translation. We analyze the rock slide initiation process using a block slide model.

Analysis

The free-body diagram in Figure 5 illustrates the situation of the rock slide block before the earthquake. The force normal to the slope is $mg \cos \delta$, where m is the mass of the free-body, g is the gravitational acceleration, and δ is the dip angle. A basal friction force $\mu_s mg \cos \delta$ balances the $mg \sin \delta$ downhill force generated by gravity, and

$$mg \sin \delta < \mu_s mg \cos \delta + cA, \qquad (1)$$

where μ_s is the coefficient of static friction, c is the cohesive strength across the sliding surface, and A is the area of the sliding surface. (Because of the many joints observed in the

Figure 4. Photograph showing part of a rockslide at Jih-Feng-Erh-Shan (looking from the head scarp). The sliding layer of Changhukeng Shale measures 30 to 50 m thick.

shale layer, we assume that the rock mass was well drained before the earthquake and neglect the pore-pressure effect in the rock slide initiation problem considered here.) Take the cohesion of an intact shale of 1.44×10^4 N/m^2 (Wieczorek *et al.,* 1982) and a density of 2.1 g/cm^3, $cA/(mg \sin \delta) \cong 0.06$ for a 30-m thick layer and $\delta = 24°$. For sliding across an existing bedding plane, the ratio is likely to be smaller. The factor of safety (FS) (Newmark, 1965; Wilson and Keefer, 1983) is given by $FS = (\mu_s mg \cos \delta + cA)/(mg \sin \delta) > 1$. We consider next the initiation of the slide.

Figure 6 shows the mass in Figure 5 under earthquake

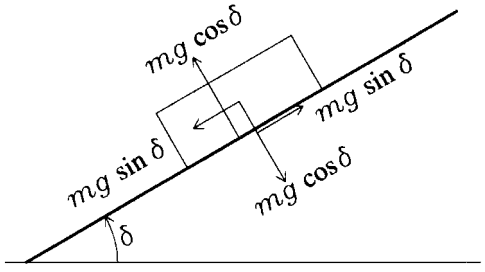

Figure 5. Free-body diagram of a balanced rock block prior to the earthquake. A $mg \cos \delta$ reaction force from the underlying bed balances the $mg \cos \delta$ force in the direction perpendicular to underlying bed generated by gravity. A $\mu_s mg \cos \delta = mg \sin \delta$ basal shear resistance balances the $mg \sin \delta$ downhill force generated by gravity; $mg \sin \delta < \mu_s mg \cos \delta + cA$, where c is the cohesive strength across and A is the area of the sliding surface. The torque of all forces adds to zero.

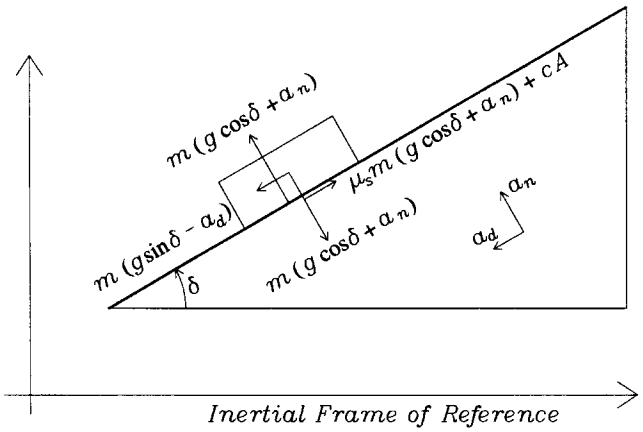

Figure 6. Free-body diagram of the rock block in Figure 12 under earthquake ground motion and critically balanced conditions. The rock block and the base of the slide (represented by the wedge) are considered to be rigid bodies. Interactions between the two rigid bodies are friction and cohesion. Relative to the inertial frame of reference, the base moves with accelerations a_n in the direction normal to the slide surface (positive away from the slope) and a_d tangential to the slide surface along the dip (positive downdip). The rock block reacts to these accelerations. Relative to the wedge, the rock block is pulled by an $m(g \cos \delta + a_n)$ equivalent gravitational force in the direction perpendicular to the sliding surface. A reaction force of magnitude $m(g \cos \delta + a_n)$ from the sliding surface balances this equivalent gravitational pull. A $\mu_s m(g \cos \delta + a_n)$ basal friction force plus a cohesive force cA counteracts the $m(g \sin \delta - a_d)$ downhill force generated by the equivalent gravity.

ground motion. The rock block and the base of the slide (represented by the wedge) are considered to be rigid bodies. The mass of the rock block is negligible compared to that of the base. Interactions between the two rigid bodies are friction, cohesion, and pore-pressure effects; we neglect the pore pressure for the rockslide initiation problem. Relative to the inertial frame of reference, the base moves with accelerations a_n in the direction normal to the slide surface (positive away from the slope), a_d tangential to the slide surface along the dip (positive down dip), and a_s tangential to the slide surface along the strike. The rock block reacts to these accelerations. Relative to the wedge, the rock block is pulled by an equivalent gravitational force $mg(\cos\delta + a_n)$ in the direction perpendicular to the sliding surface. A reaction force of magnitude $mg(\cos\delta + a_n)$ from the sliding surface balances this equivalent gravitational pull. The acceleration parallel to the strike, a_s, does not enter into the two-dimensional analysis here. When

$$(g \sin\delta - a_d) \le \mu_s (g \cos\delta + a_n) + \frac{cA}{m}, \quad (2)$$

the block is stationary. When $(g \sin\delta - a_d) > \mu_s (g \cos\delta + a_n) + cA/m$, the block slides relative to the base. Because $mg \sin\delta$ always acts in the down-dip direction, equation (2) favors down-slope sliding. Clark (1972) derived similar expression for stones displaced by earthquake ground shaking.

The components a_d, a_s, and a_n are given in terms of a_E (east acceleration), a_N (north acceleration), a_V (vertical acceleration), ϕ_s (strike angle from north), and δ by

$$\begin{aligned} a_d &= a_E \cos\delta \cos\phi_s - a_N \cos\delta \sin\phi_s - a_V \sin\delta, \\ a_s &= a_E \sin\phi_s + a_N \cos\phi_s, \\ a_n &= a_E \sin\delta \cos\phi_s - a_N \sin\delta \sin\phi_s + a_V \cos\delta. \end{aligned} \quad (3)$$

There are no acceleration records at the rockslide. For illustration, we calculate the down-dip sliding acceleration, $S = (g \sin\delta - a_d) - \mu_s (g \cos\delta + a_n) - cA/m$, using the records at the nearest strong-motion station TCU089 (23.9037° N, 120.8565° E and 6.7 km away from the landslide). When $S > 0$, rock slide motion can be initiated.

Results

Figure 7 shows the vertical, north–south, and east–west component of the acceleration records. Figure 8 shows the components resolved in directions normal to the slide surface, tangential to the slide surface down-dip, and tangential to the slide surface parallel to the strike where we have used the minimum dip angle, $\delta = 18°$, in the Central Geological Survey (2000) report for calculation. From equation (3) and $\cos\delta = 0.95$, $\sin\delta = 0.31$, a_v contributes mainly to a_n. The top two figures in Figure 9 show the down-dip sliding accelerations calculated with a_n, S (top figure), and those without a_n, $S1$ (middle figure), for $\mu_s = 0.466 = \tan 25°$ and $cA/(mg \sin\delta) \cong 0.05$. Results calculated without a_n, $S1$, correspond to those calculated by the Newmark method (Newmark, 1965), currently widely used for the slope-stability analysis. The bottom figure shows that $S - S1 > 0$ when $S > 0$ or $S1 > 0$, and the ratio $(S - S1)/S$ can be greater than 50%. For our example, the onset of $S > 0$ occurs ~4 sec earlier when a_n is included. From equation (2), the larger μ_s is, the larger is the effect of a_n on the sliding acceleration.

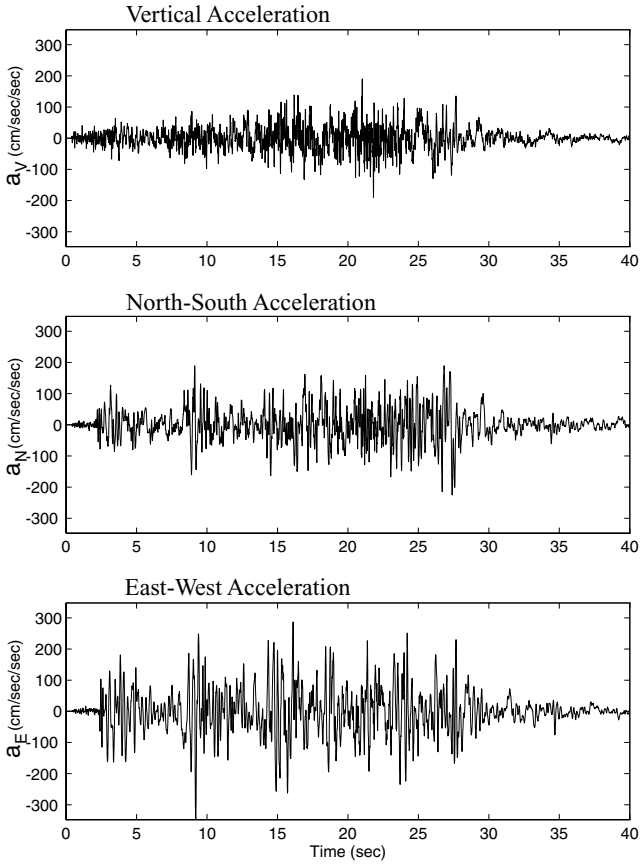

Figure 7. The vertical, north–south, and east–west component of the acceleration records from a strong-motion station about 7 km southeast of the rockslide.

If we use the larger dip angle in the Central Geological Survey (2000) report, $\delta = 24°$, in our calculation, the sliding acceleration results are as shown in Figure 10. The slope angle is so close to the friction angle of 25° that the rockslide is easily triggered. The effect of a_n is smaller in this case; $(S - S1)$ is no longer strictly positive when $S > 0$ or $S1 > 0$, but the majority of positive peaks of S have larger amplitude than those of $S1$.

Newmark (1975) introduced a critical displacement, required for a loss of strength sufficient to allow large-scale failure, for artificial embankments. Wilson and Keefer (1983) adapted the critical displacement to natural slopes: "For natural slopes, this critical displacement could vary widely, depending on the mechanism of slope failure (fall, slump, block slide, etc.), lithology, slope geometry, and pre-

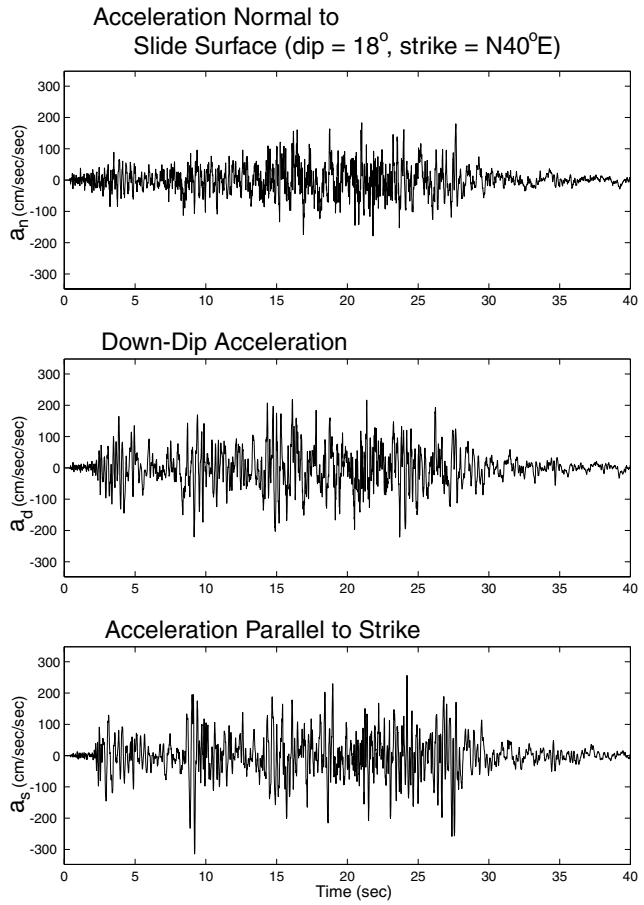

Figure 8. Acceleration components normal to the slide surface, in the down-dip direction, and parallel to the strike, calculated from the acceleration records in Figure 7.

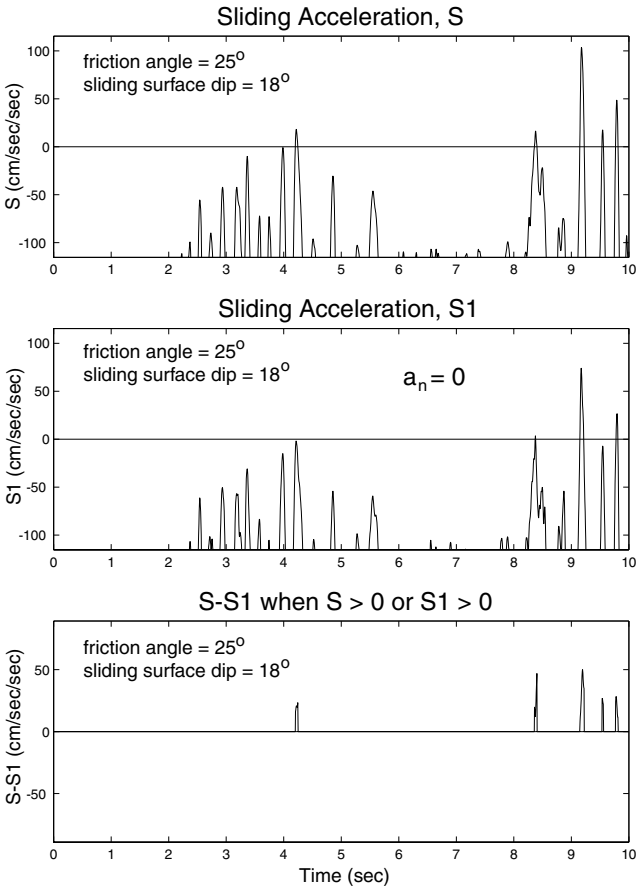

Figure 9. Down-dip sliding acceleration calculated with and without the acceleration component normal to the sliding surface. The dip angle of the sliding surface is 18°.

vious history of slope movement." We calculate the rockslide displacement under the sliding acceleration S by substituting S for $a(t) - a_c$ as done by Wilson and Keefer (1983). The algorithm that we use was described by Jibson (1993).

For the case of a slide surface dipping 18°, a Newmark analysis that accounts for a_n (S, top of Fig. 9) yields a displacement $d_S = 0.48$ cm. An analysis that neglects a_n ($S1$, middle of Fig. 9) yields a displacement of $d_{S1} = 0.20$ cm. For the steeper dip angle of 24°, the Newmark displacements calculated for S and $S1$ in Figure 10 are $d_S = 19.19$ cm and $d_{S1} = 11.49$ cm, respectively. Thus, including the effects of seismic accelerations normal to the slide surface in the Newmark analysis roughly doubles the estimated Newmark displacements.

Discussion and Conclusions

Two parameters used in our analysis, the coefficient of friction, μ_s, and the cohesion, c, at the interface of the Changhukeng Shale and the underlying Shihmen Sandstone are unknown. We showed in the Analysis section that, using a cohesion value of 1.44×10^4 N/m^2 (that of an intact shale), the magnitude of the resisting force from cohesion is 0.06 of that of the driving gravitational force. Uncertainty in c can therefore cause only second-order changes in the results. By varying the coefficient of friction, we found that the condition $S > 0$ occurs for μ_s as high as 0.73 on a 24°-dip slope.

We have analyzed the initiation of the rockslide avalanche at Jih-Feng-Erh-Shan using Newmark's (1965) sliding-block model. Although this model is highly simplified and does not account for such factors as internal deformation of the slide block, variation of acceleration over the slide area, and pore-pressure effects along the sliding surface, it is widely used to estimate the performance of slopes during earthquake shaking. Standard applications of Newmark's method neglect ground accelerations normal to the slide surface. We conducted comparative analyses of conditions both with and without slope-normal accelerations; our results show that including slope-normal accelerations roughly doubles the estimated Newmark displacement, which in many cases could lead to a significant different estimate of overall slope performance.

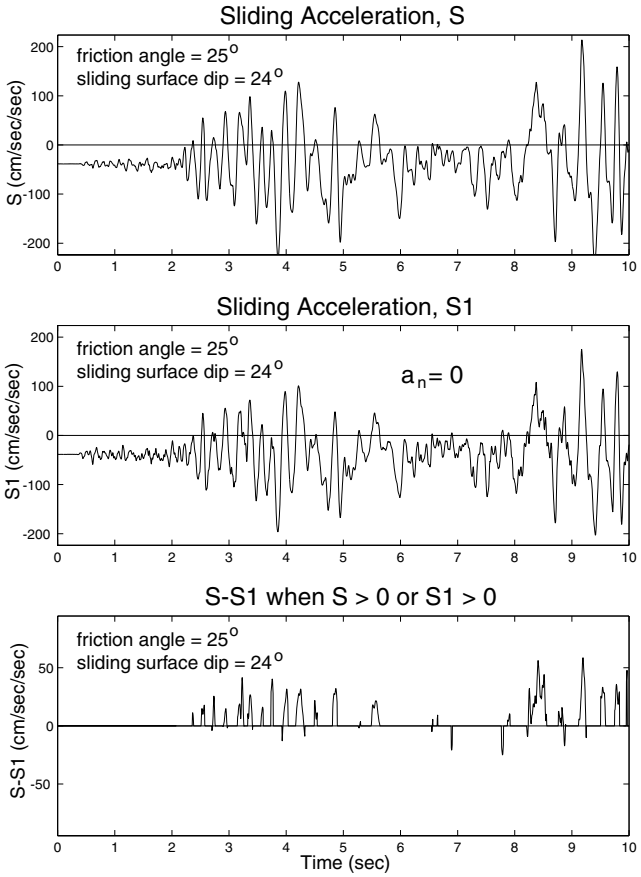

Figure 10. Down-dip sliding acceleration calculated with and without the acceleration component normal to the sliding surface. The dip angle of the sliding surface is 24°.

Acknowledgments

Three of us (H.-P. L., D. K. K., and R. W. J.) visited the field sites in January of 2000. We thank our host at the Central Geological Survey (Director Chao-Hsia Chen, Dr. Hui-Cheng Chang, and Messrs. Wei-Yu Wu, Jiin-Fa Lee, Shyun-Sheng Chang Tung-Sheng Shih, and Shih-Lin Lee). We also thank our colleagues at the National Taiwan University—professors Yue-Gao Chen, Ching-Hua Lo, Cheng-Hong Chen, and Wen-Shan Chen—and at the National Central University—professors Yi-Ben Tsai, Chyi-Tyi Lee, Kuo-Fong Ma, Kuo-Liang Wen, and Chien-Ying Wang—for information on the Chi-Chi earthquake. We thank the Central Weather Bureau of Taiwan and Dr. William H. K. Lee of the USGS, who provided us with the digital strong ground motion accelerometer records of the Chi-Chi earthquake. Review comments by Dr. David M. Boore, Mr. Richard E. Warrick, and two anonymous reviewers improved our manuscript.

References

Central Geological Survey (2000). Investigative Report on the Earthquake Geology of the September 21 Earthquake, Central Geological Survey, The Ministry of Economic Affairs, Taiwan, Republic of China (in Chinese).

Clark, M. M. (1972). Intensity of shaking estimated from displaced stones, in *The Borrego Mountain Earthquake of April 9, 1968, U.S. Geol. Surv. Profess. Pap. 787,* 175–182.

Jibson, R. W. (1993). Predicting earthquake-induced landslide displacements using Newmark's sliding block analysis, Transportation Research Board, Transportation Research Record 1411, 9–17.

Kamai, T., W. N. Wang, and H. Shuzui (2000). The landslide disaster induced by the Taiwan Chi-Chi earthquake of 21 September 1999, *Landslide News* **13,** 8–12.

Ho, C. S. (1988). *An Introduction to the Geology of Taiwan, Explanatory Text of the Geologic Map of Taiwan,* Second Ed., Central Geologic Survey, The Ministry of Economic Affairs, Taiwan, Republic of China.

Lee, W. H. K., T. C. Shin, K. W. Kuo, and K. C. Chen (1999). CWB Free-Field Strong-Motion Data from the 21 September Chi-Chi, Taiwan, Earthquake, digital acceleration files on CD-ROM, Vol. 1.

Ma, K.-F., C.-T. Lee, Y.-B. Tsai, and T. C. Shin (1999). The Chi-Chi, Taiwan earthquake: large surface displacements on an inland thrust fault, *EOS Trans. AGU* **80,** no. 50.

Newmark, N. M. (1965). Effects of earthquakes on dams and embankments, *Geotechnique* **15,** 139–160.

Shin, T. C., K. W. Kuo, W. H. K. Lee, T. L. Teng, and Y. B. Tsai (2000). A preliminary report on the 1999 Chi-Chi (Taiwan) earthquake, *Seism. Res. Lett.* **71,** 24–30.

Wieczorek, G. F., R. C. Wilson, and E. L. Harp (1982). Map showing slope stability during earthquakes in San Mateo County, California, *U.S. Geol. Surv. Misc. Invest. Ser. Map,* Map I-1257-E, scale 1:62,500.

Wilson, R. C., and D. K. Keefer (1983). Dynamic analysis of a slope failure from the 6 August 1979 Coyote Lake, California, earthquake, *Bull. Seism. Soc. Am.* **65,** 1239–1257.

Central Geological Survey
No. 2, Lane 109, Huahsin Street
Chungho Taipei, Taiwan
huangcc@linx.moeacgs.gov.tw
dljp@linx.moeacgs.gov.tw
(C.-C.H., Y.-H.L.)

U.S. Geological Survey
MS 977
345 Middlefield Road
Menlo Park, California 94025
liu@usgs.gov
dkeefer@usgs.gov
(H.-P.L., D.K.K.)

U.S. Geological Survey
Box 25046, MS 966
Denver Federal Center
Denver, Colorado 80225
jibson@usgs.gov
(R. W. J.)

Manuscript received 24 August 2000.